ChemPubSoc Europe

DOI: 10.1002/open.201600159

Open Access ChemistryOPEN Full Papers

Synthesis, Characterization, and Antimicrobial Activity of Near-IR Photoactive Functionalized Gold Multibranched Nanoparticles

Yevgeniya Kalachyova,[a, b] Anasiya Olshtrem,[d] Olga A. Guselnikova,[a, b] Pavel S. Postnikov,[b] Roman Elashnikov,[a] Pavel Ulbrich,[c] Silvie Rimpelova,[c] Václav Švorčík,[a] and Oleksiy Lyutakov*[a, b]

Surface-modified gold multibranched nanoparticles (AuMs) were prepared by simple chemical reduction of gold chloride aqueous solution followed by in situ modification by using water-soluble arenediazonium tosylates with different functional organic groups. Chemical and morphological structures of the prepared nanoparticles were examined by using transmission electron and scanning electron microscopies. The covalent grafting of organic compounds was confirmed by scanning electron microscopy with energy dispersive X-ray spectroscopy (SEM-EDX) and Raman spectroscopy techniques. Covalent functionalization of nanoparticles significantly expands the range of their potential uses under physiological conditions, compared with traditional non-covalent or thiol-based approaches. The antibacterial effect of the surface-modified AuMs was evaluated by using *Escherichia coli* and *Staphylococcus epidermidis* bacteria under IR light illumination and without external triggering. Strong plasmon resonance on the AuMs cups leads to significant reduction of the light power needed kill bacteria under the mild conditions of continuous illumination. The effect of the surface-modified AuMs on the light-induced antibacterial activities was founded to be dependent on the grafted organic functional groups.

1. Introduction

The increasing prevalence of bacterial strains resistant to widely used antibiotics is one of the most relevant problems in medicine for which an urgent solution is needed.[1,2] Therefore, new types of antibacterial compounds and effective therapeutic strategies should be developed to solve this growing problem.[3,4] Metal nanoparticles (MNPs) (e.g., silver, copper, gold) provide versatile platforms for therapeutic applications based on their physical properties.[5] In particular, AgNPs are very effective against bacteria strains.[6,7] However, there are many concerns over their cyto- and genotoxicity toward mammalian cells.[8,9] Thus, the use of AgNPs in the medical field is limited because of possible damage to the surrounding healthy tissue. However, there is one type of NPs that, compared with other NPs, exhibits low toxicity and seems to be "cytocompatible": nanoparticulate gold (AuNPs).[10] Unfortunately, the size- and shape-dependent[11,12] antibacterial activity of AuNPs as such is not sufficient.[13]

To overcome this issue, surface functionalization of AuNPs was proposed. Grafting of various molecules on the AuNPs surface facilitates their binding to the bacterial membrane and makes it easier to kill the bacteria. In particular, the simple immobilization of charged molecules on the AuNPs surface can significantly increase their antibacterial activity.[14] Very promising is the binding of antibiotic molecules to AuNPs, which not only shows a synergetic effect but overcomes the antibiotic resistance too.[15–17] AuNPs have been also combined with another class of antibacterial agents—quaternary ammonium salts[18]—or capped with naturally non-antibacterial chelators, which destroy the bacterial membrane through the expropriation of bivalent cations.[19] Thus-functionalized AuNPs are now being widely investigated owing to their antibacterial, antibiofilm, and antifungal activity.[20]

Besides their cytocompatibility and easy surface functionalization, AuNPs exhibit apparent absorption of near-IR light (NIR) as a result of efficient plasmon excitation. Treatment with

[a] *Y. Kalachyova, O. A. Guselnikova, R. Elashnikov, Prof. Dr. V. Švorčík, Dr. O. Lyutakov*
Department of Solid State Engineering
University of Chemistry and Technology
Prague 166 28 (Czech Republic)
E-mail: lyutakoo@vscht.cz

[b] *Y. Kalachyova, O. A. Guselnikova, Dr. P. S. Postnikov, Dr. O. Lyutakov*
Department of Technology of Organic Substances and Polymer Materials
Tomsk Polytechnic University
634050 Tomsk (Russia)

[c] *Prof. Dr. P. Ulbrich, Dr. S. Rimpelova*
Department of Biochemistry and Microbiology
Institute of Chemical Technology
166 28 Prague (Czech Republic)

[d] *A. Olshtrem*
Department of Bioengineering and Organic Synthesis
Tomsk Polytechnic University
634050 Tomsk (Russia)

NIR light is very interesting and promising in the medical field, as laser irradiation with NIR light can be optimized to provide minimum damage to the tissue. From this point of view, light absorption by functional AuNPs and photothermal damage to cells is currently one of the most promising research avenues in the treatment of cancer and infectious diseases.[21–23] This method of therapy, first introduced by Pitsillides et al.[24] and further developed by Zharov et al.[25] and Khlebstov et al.,[26] is usually called plasmonic photothermal therapy and represent an alternative approach for antibiotics treatment or cancer chemotherapy.[27,28] Various functionalized AuNPs have been tested for their light-induced antibacterial activity.[26] It was found that single AuNPs with spherical shape are relatively ineffective. However, by changing the AuNPs shape to nanorods,[29,30] nanoshells,[31,32] or nanocages[33] can lead to efficient light-activated antibacterial materials.[34,35]

As NIR light is capable of penetrating deeper tissues, NPs capable of absorbing NIR light are postulated to be suitable for use as photothermal agents in vivo.[36] However, standard thiol chemistry or non-covalent binding of functional molecules to the AuNPs surface is not the best choice for in vivo conditions for several reasons: the increased ion strength can disrupt the non-covalent interaction; the thiol groups from in vivo occurred peptides can substitute the functional groups on the AuNPs surface; and finally, the Au–C bonds are stronger than Au–S (the binding energy of the aryl layer on gold is higher by 14.2 kJ mol^{-1} than that of the thiol).[37,38]

To the best of our knowledge, most work in the field of gold nanoparticles functionalization has used the thiol approach. However, temperature increases or laser illumination associated with the use of AuNPs for phototherapy can disrupt the thiol bonds, leading to the loss of nanoparticle activity.[39] In this work, attempts to perform surface functionalization of gold multibranched nanoparticles through diazonium chemistry were made.[40,41] An alternative diazonium approach can create covalent bonds between the gold surface and organic compounds, preventing the detachment or substitution of the grafted organic functional groups.[42] For these reasons, the diazonium approach is becoming increasingly popular in the medical field.[43] Such created functional nanoparticles seem to be an efficient agent for phototherapy, and can substitute the traditional thiol-functionalized nanoparticles. Additionally, a new class of AuNPs—so-called multibranched nanoparticles (AuMs), with extremely high numbers of plasmonic hot spots per single nanoparticle, are used. Their application allows us to activate antibacterial activity under "extremely" mild light illumination conditions.

2. Results and Discussion

A schematic representation of the multibranched gold nanoparticles (AuMs) synthesis and surface modification is given in the Figure 1. AuMs were synthesized in aqueous solution at room temperature according to the described procedure.[44] The formation of branches on the gold surface is explained by the presence of silver ions, which induced the anisotropic growth of gold. Prepared AuMs were surface modified by several arenediazonium tosylate (ADTs) salts with the aim of changing the surface charge of the NPs and introducing functional groups. The modification of the nanoparticle surface was carried out by interaction of the freshly prepared suspension of AuMs with water solutions of arenediazonium tosylates (ADTs): 4-nitrobenzenediazonium tosylate, 4-aminobenzenediazonium tosylate, and 4-carboxybenzenediazonium tosylate. After addition of the diazonium solution to the AuMs suspension, we observed evolution of nitrogen as an indirect indication of the modification process.

Figure 1. Synthesis of modified gold multibranched nanoparticles (mod-AuMs-R; R = –COOH, $–NH_2$, $–NO_2$).

The AuMs shape and size distribution were examined by using SEM and TEM after preparation and purification procedures. The results are presented in Figure 2. From Figure 2a it is evident that the applied NPs synthesis procedure leads to the formation of AuMs, with a greater number of curved edges. TEM analysis (Figure 2b) revealed spiky star-shaped crystals. The AuMs size distribution lies in the 30–60 nm range, which is typical for this new kind of AuNP.[44] It should be noted that the large number of curved objects on the NPs surface leads to very effective plasmon excitation (so-called hot spots in plasmonics) and light energy focusing through the photon–plasmon conversion on these hot spots. Excited plasmons can focus the energy of incident plasmons to the very

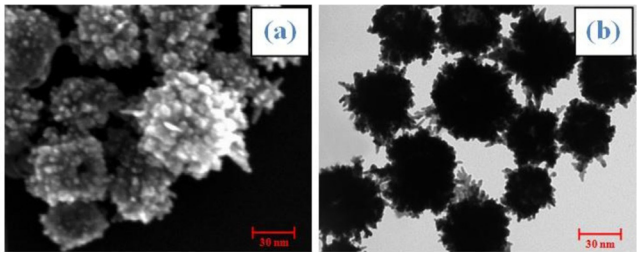

Figure 2. a) SEM and b) TEM images of modified gold multibranched nanoparticles.

small volume, close to the shaped NP edge. Simultaneously, the distinctly non-spherical shape of the AuMs presents a chemically active background for further surface modification.

Surface modification of AuMs was performed in water solution, through diazonium chemistry with the aim of introducing on the NPs surface organic functional groups, able to interact (bind) with bacterial membranes. The first observation, indirectly confirming the AuMs–ADT interaction, was the evolution of nitrogen from the reaction solution. Another confirmation lies in the significant increase of AuMs stability after their surface modification. Convincing proof is provided by the photos of AuMs vials, taken after 48 h of their storage under ambient conditions, which are shown in Figure 3. From the change of the solution color, it is evident that during storage, the non-

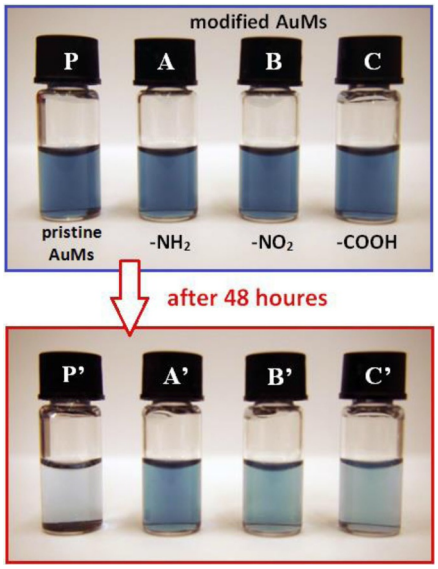

Figure 3. Photos of pristine (P) and functionalized AuMs A–C) freshly prepared and A′–C′) after storage (48 h, P′) at ambient conditions.

modified AuMs segregate and sediment and the solution becomes transparent. The aqueous dispersion of modified AuMs, however, was found to be stable against AuMs aggregation and sedimentation. The original solution color is conserved for 48 h. It may be concluded that surface modification of AuMs by ADTs increase the stability of the dispersion, this finding correlates with previously published work dedicated to the stabilization of AgNPs by diazonium salts.[45] Improved dispersibility could positively affect the antibacterial properties of AuMs. A similar approach for increasing the MNPs water solubility and suspension stability through the formation of metal–carbon σ-bonds.[45]

The results of AuMs surface modification and organic functional group (OFG) grafting were also checked by using Raman spectroscopy (SERS = surface enhanced spectroscopy mode) and SEM-EDX analysis. The results of the SEM-EDX analysis are presented in Figure 4. Here, the top row gives the SEM images of pristine and modified AuMs, the lower rows show the spatial distribution of "organic" elements on the NP surfaces. The

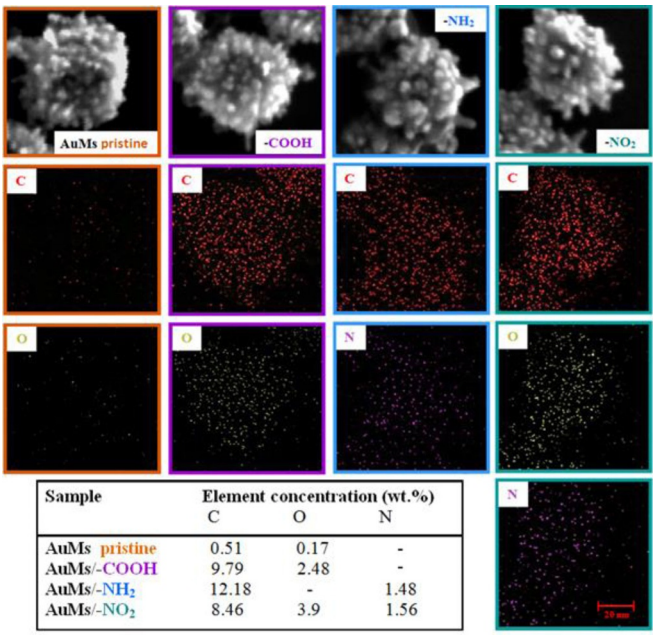

Sample	Element concentration (wt.%)		
	C	O	N
AuMs pristine	0.51	0.17	-
AuMs/-COOH	9.79	2.48	-
AuMs/-NH_2	12.18	-	1.48
AuMs/-NO_2	8.46	3.9	1.56

Figure 4. EDS analysis of pristine and modified (–COOH, $-NH_2$, and $-NO_2$) gold multibranched nanoparticles. The weight concentrations of organic elements are summarized in the table.

element concentrations, determined from EDX spectra, are given in the underlying table. First, it must be noted that only negligible concentrations of organic elements were detected on the pristine AuMs. Their presence can be attributed to contamination by carbon from air or partial oxidation of the metal. SEM measurements indicate that after modification no significant changes in AuMs shape and size were detected (compare with Figure 2). Then, EDS analysis confirmed the presence of OFGs on the NP surfaces with a spatial distribution correlating to the physical positions of AuMs on the SEM scans. The element ratio values correlate with the composition of the attached OFGs. Additionally, a much lower presence of "organic" elements in the maps measured for the pristine, nongrafted AuMs clearly indicates the removing of citrate groups.

The presence of OFGs was also detected by Raman spectroscopy (Figure 5). As the AuMs contain a large number of plasmonic hot spots, a significant enhancement of grafted OFGs Raman response can be expected. From Figure 5 it is evident that a perfect SERS response, with excellent signal to noise ratio, was obtained. In particular, the SERS spectra identify the presence of all grafted OFGs: 4-nitrophenyl (-C_6H_4-NO_2), 4-aminophenyl (-C_6H_4-NH_2), and 4-carboxyphenyl (-C_6H_4-COOH). The characteristic bands for all grafted OFGs are summarized in Table 1. It should be also strongly stressed that an additional peak at $\approx$400 cm^{-1} appears for all functionalized samples and confirms the formation of covalently attached organic functional groups.[46–48] This fact is especially important owing to the potential application of functionalized AuMs in in vitro conditions, where the traditionally used non-covalent or thiol chemistry functionalization can be displaced or substituted with subsequent loss of functional NP activity. From the Raman measurements, the excellent SERS activity as a result of

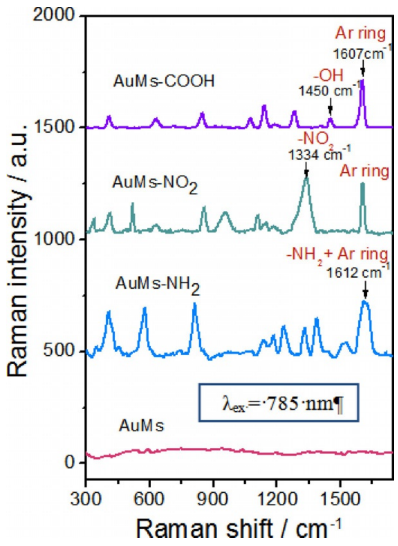

Figure 5. Raman spectra of multibranched nanoparticles (AuMs) and surface-modified gold multibranched nanoparticles (mod-AuMs) by ADTs with $-NO_2$, $-NH_2$, –COOH functional groups (aromatic ring = Ar).

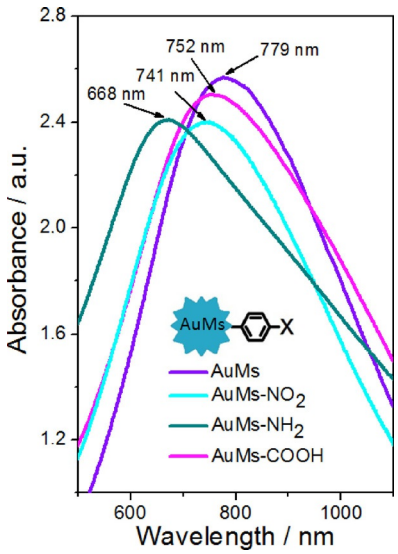

Figure 6. UV/Vis spectra of multibranched nanoparticles (AuMs) and surface-modified gold multibranched nanoparticles (mod-AuMs) by ADTs with $-NO_2$, $-NH_2$, –COOH functional groups.

Table 1. Raman peak frequencies and assignments for AuMs modified with ADTs.

Assignments	Band position [cm^{-1}]
Au–C stretch	404–410[46–48]
NO_2 rocking	530–570[60,61]
Ar ring stretch	630–650[60,61]
NH_2 wag	814[62,63]
ONO scissor + Ar ring stretch	850–860[60,61]
C–H in-plane bend	1020–1080[60,61]
C–N stretch + Ar ring stretch	1100–1280[60–63]
O–H in-plane bend	1140–1550[64]
C–N stretch	1110–1230[62,63]
Ar ring stretch	1330–1400[60,61]
NO_2 symmetric stretch	1335[60,61]
NH_2 stretch, Ar ring stretch	1520–1620[60–63]
C=O stretch	1607[64]

the AuMs shape ensured significant light intensity increase,[49] which can be exploited for existing and some fascinating potential applications of plasmonic NPs in the medical area, applications that require higher deposited photon energy to achieve the required therapeutic effect. Additionally, the absence of the apparent peaks in the Raman spectrum, measured for the pristine, nongrafted AuMs indicate the removal of all citrate groups during the three-time repeated purification procedure.

The UV/Vis absorption spectra of pristine and surface-grafted AuMs in water solution are represented in Figure 6. From the absorption spectrum of pristine AuMs it is evident that their optical properties are dominated by the plasmon tip modes.[50] The localized surface plasmon resonance (LSPR) occurring at 780 nm can be strongly tip-associated, indicating the strong energy focusing of the shaped edges of AuMs. This is also accompanied by a visible change in the solution, the color of which is dark blue owing to plasmon peak redshifts (Figure 3). Additionally, Figure 6 shows the UV/Vis spectra of the modified nanourchins with absorption maxima shifted to lower wavelengths for samples modified by ADTs with $-NO_2$, $-NH_2$, and –COOH functional groups. It is evident that the surface functionalization shifts the position of LSP significantly. It could be expected that the position of LSP is a function of the dielectric environment, that is, that the OFGs grafting changes the dielectric function of the plasmon environment. For antibacterial treatment, the plasmon excitation at the highest wavelength of 780 nm is of particular interest. From Figure 6 it is evident that surface functionalization affects the wavelength position but the absolute value of the absorption coefficient indicates that LSP can be still sufficiently excited.

According to published data, AuNPs exhibit promising levels of toxicity, but also low antibacterial activity. Their antibacterial activity can be enhanced by changing the AuNP shape, or by combination with antibiotics, surface functionalization, or laser triggering. In the usual experimental arrangement, the triggering of AuNPs antibacterial activity by IR laser illumination requires the application of short laser pulses to prevent heat diffusion from the absorbed AuNPs and at the same time to destroy the bacterial membrane faster before the AuNPs cool down.[51] Recently, antibacterial activity was also achieved under continuous laser treatment through the substitution of traditional spherical AuNPs by NPs with polygonal shape.[52] In this case, of special interest is the AuNPs surface functionalization with the aim of increasing AuNPs affinity for the bacterial membrane combined with light triggering to destroy the membrane and to kill the bacteria.

In the next experiments, we apply both strategies and the new type of AuMs. Enhancement of the MNPs antimicrobial activity through diazonium chemistry based functionalization was also reported in a previous work.[45] The results of the antibacterial tests are presented in Figure 7 and Table 2, which show the number of surviving bacteria (measured as CFU = colony founded units) after their incubation with pristine and

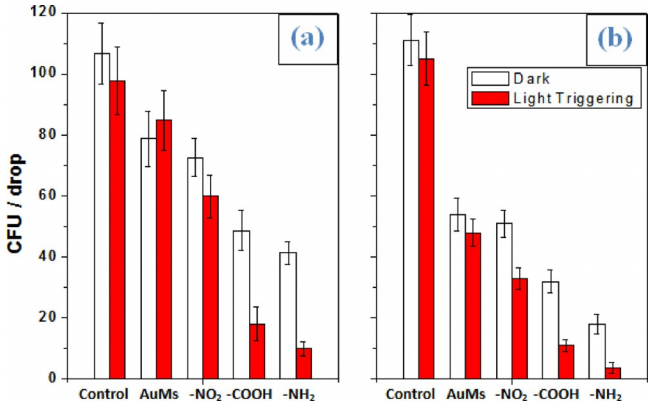

Figure 7. Antimicrobial activity: CFU per mL after bacteria incubation with a) *E. coli* or b) *S. epidermidis* with AuMs and differently modified AuMs (with $-NO_2$, $-NH_2$, –COOH) with and without light triggering.

Table 2. Antimicrobial activity: CFU per mL after bacteria incubation with a) *E. coli* or b) *S. epidermidis* with AuMs and differently modified AuMs (with $-NO_2$, $-NH_2$, –COOH) with and without light triggering.

Sample	*E. coli*		*S. epidermidis*	
	dark	light	dark	light
Control	106.5 ± 10	97.8 ± 11	111.9 ± 10.1	105.3 ± 9.1
AuMs	78.7 ± 9.2	84.9 ± 9.2	56.9 ± 5.2	50 ± 5.1
$-NO_2$	72.6 ± 6.1	59.9 ± 6.9	54.2 ± 4.8	35.3 ± 3.9
–COOH	48.6 ± 6.6	18.1 ± 5.4	34.1 ± 2.5	10.1 ± 2.4
$-NH_2$	41.3 ± 3.8	10 ± 2.4	18.1 ± 2.7	4.3 ± 1.9

surface-functionalized AuMs with and without IR illumination. From Figure 7 it is evident that the light treatment results in only a slight decrease in surviving bacteria but the effect is almost negligible. Incubation of bacterial strains with nonfunctionalized AuMs results in bacteria death. This effect is apparent in the case of gram-positive *Staphylococcus epidermidis* (Figure 7 b) but it is very weak in the case of gram-negative *Escherichia coli* (Figure 7 a). Surface functionalization of AuMs increases their antibacterial activity. This effect can be attributed to facilitation of the nanoparticles–antimicrobial membrane interaction, as a result of the presence of amino and carboxyl groups on the AuMs surface. It is well known that the grafting of carboxyl or amino groups onto an antimicrobial agent can improve its interaction with the membranes of bacterial cells.[53,54] In the present case, a more pronounced antimicrobial effect was achieved for gram-positive bacterial strains. As can be expected, the effect depends on the functional groups present: grafting with amino groups results in the best antibacterial activity, grafting with carboxyl OFGs also leads to an increase of antibacterial activity, but the nitro OFGs practically does not change the antibacterial activity of the AuMs. As is apparent from Figure 7, the antibacterial activity of functionalized AuMs can be significantly increased by intervention of an external energy source, that is, light illumination close to the LSP wavelength. The most effective bacteria killing was achieved in the case of amino-grafted AuMs where almost full bacteria deactivation was achieved. Slightly worse, but still effective deactivation was achieved in the case of carboxyl-grafted AuMs. A positive effect of light treatment was also found for the AuMs grafted with OFGs. In all cases, gram-negative *E. coli* showed better resistance than gram-positive *S. epidermidis* to antibacterial triggering. It must be noted that we applied rather a mild intensity of IR light and continuous light illumination. The application of AuMs together with effective plasmon excitation concentrates efficiently the light energy into so-called hot spots on the NPs cups and leads to strong and efficient degradation of neighboring organic compounds and destruction of the bacterial membrane. In this case, the short laser pulses can be substituted by strong LSP excitation, resulting in efficient triggering of antibacterial activity under mild conditions (light power and continuous illumination).

3. Conclusions

This work describes the synthesis and surface functionalization of Au multibranched nanoparticles (AuMs) with different functional groups covalently grafted on the Au surface. Synthesis of the multibranched NPs was performed through particular spatial blocking of Au seeds by silver and anisotropic growth of gold. The covalent grafting of organic functional groups was realized by using diazonium chemistry. The results of the AuMs synthesis and their functionalization were checked by using TEM, SEM-EDX, SERS, and UV/Vis spectroscopy techniques. The as-prepared AuMs exhibited low antibacterial activity, which is significantly increased by the grafting of carboxyl and amino functional groups onto their surfaces. Light triggering of these functional AuMs further increases their efficiency in the killing of both gram-negative and gram-positive bacteria. This significant increase of AuMs bioactivity was achieved under the illumination at "tissue-favorable" IR wavelengths and under very mild illumination conditions. This type of AuMs with a wide range of attached functional groups and in combination with light treatment has huge potential for applications in antibacterial treatment and cancer therapy. Contrary to other studies where electrostatic or thiol-chemistry approaches were used for the attachment of organic functional groups, in this work primary covalent grafting of organic compounds was applied. In the former case, reduction of the electrostatic interactions or thiol-linked compounds substitution under in vivo physiological conditions make the functional materials significantly less stable and lead to reduction of their antibacterial activity. The present method is free of such weaknesses and it gives a favorable opportunity to the creation of functional metal AuMs for in vivo phototherapy and other medical applications.

Experimental Section

Materials

Chloroauric acid tetrahydrate ($HAuCl_4 \cdot 4H_2O$, 99.9%), silver nitrate ($AgNO_3$, 99.0%), ascorbic acid (AA, 99.0%), *p*-toluenesulfonic acid monohydrate (98.0%), acetic acid (≥99.7%), *tert*-butyl nitrite (90.0%), 4-nitroaniline (≥99%), 4-aminobenzoic acid (≥99%), 4-aminoaniline (≥99.0%), and diethyl ether (≥99.7%) were purchased from Sigma–Aldrich. All chemical reagents were used as re-

ceived without further purification. Mueller–Hinton agar (MHA) was prepared as described by the producer (Oxoid, CM0337) and sterilized in an autoclave. Deionized water was used throughout the experiments. The corresponding arenediazonium tosylates (4-nitrobenzenediazonium tosylate, 4-aminobenzenediazonium tosylate, and 4-carboxybenzenediazonium tosylate) were prepared according to the described procedure.[55]

Preparation of Multibranched (Urchin-like) Gold NPs

Au multibranched NPs (AuMs) were synthesized by a known procedure.[44] Aqueous $HAuCl_4$ solution (100 μL, 10 mM) was mixed with deionized water (3 mL), and then aqueous $AgNO_3$ solution (6 μL, 10 mM) was added under magnetic stirring for 30 s. After the solutions had been thoroughly mixed, ascorbic acid (2 μL, 100 mM) was "quickly" added, and the solution was stirred vigorously for 10 s at room temperature (RT). When the reducing agent was added, the color of the mixture changed immediately from yellow to dark blue, indicating the formation of AuMs. Then, the AuMs were dispersed in water (3 mL) and were purified three times by centrifugation at 5000 rpm for 10 min. For further use, the resultant precipitates were re-dissolved in deionized water.

Grafting of Organic Compounds to Nanoparticle Surfaces

An aqueous solutions of the desired arenediazonium tosylate (70 μL, 10 mM; 4-nitrobenzenediazonium tosylate, 4-aminobenzenediazonium tosylate, or 4-carboxybenzenediazonium tosylates) was added to a freshly prepared suspension of AuMs (diazonium salts preparation procedure is describe in previous works).[56,57] The mixtures were stirred for 5 min. The nanoparticles were then collected and washed thoroughly by several centrifugations at a speed of 5000 rpm for 10 min by using deionized water (1×), water/methanol (1×, 40:60), and then drying at room temperature. After the modification process, AuMs were collected by centrifugation, washed sequentially by using water, a water/methanol mixture, and methanol to remove 4-toluenesulfonic acid, unreacted diazonium salt, and its reduction products (nitrobenzene, aniline, and benzoic acid) derived from generated aryl radicals (*p*-TsOH, ADTs are soluble in water and reduction products are soluble in methanol). This washing procedure needs to be done to ensure that any organic material adsorbed on the surface is removed.[58,59]

Characterization

Transmission electron microscopy (TEM) images of the nanoparticles were obtained with a JEOL JEM-1010 instrument (JEOL Ltd., Japan), with a SIS MegaView III digital camera (Soft Imaging Systems, acceleration voltage 80 kV) and analysis was performed by using AnalySIS Software 2.0.

Scanning electron microscopy (SEM) (LYRA3 GMU, Tescan, CR) was used for the study of morphology and distribution of the modified AuMs. The nanoparticles were deposited on Si substrate and the SEM images and elemental composition and mapping were performed by using energy dispersive spectroscopy (EDS, analyzer X-MaxN, 20 mm^2 SDD detector, Oxford Instruments). The samples were attached by carbon conductive tape to avoid sample charging. SEM-EDS and SEM measurements were carried out by using accelerating voltages of 10 kV and 2 kV, respectively.

UV/Vis absorption spectra were measured by using a Lambda 25 UV/Vis/NIR Spectrometer (PerkinElmer, USA) in the spectral range 300–900 nm at a scanning rate of 240 nm min^{-1} and a data collection interval of 1 nm. The solutions were kept in 1 cm quartz cells. The reference spectrum of the solvent (deionized water) was subtracted from all spectra.

Raman scattering was measured with a Dimension-P1 Raman spectrometer (laser power 2.2 mW, integration time 1 s, frames averaged per measurement 250) with 785 nm excitation wavelength (Lambda Solutions, Inc., USA). Before sample collection, the pristine and grafted AuMs were deposited on Si substrate by using the drop-dried method. All spectra were baseline-corrected by subtracting the spectrum of pure substrate followed manual alignment of the background.

Antibacterial Tests

The antibacterial activities of pristine and surface-modified AuMs were evaluated against two environmental bacterial strains: Gram-negative *Escherichia coli* (*E. coli*, DBM 3138) and gram-positive *Staphylococcus epidermidis* (*S. epidermidis*, DBM 3179). For evaluation of antimicrobial activity in the dark, the bacteria were incubated with AuMs in the dark for 2 h. Estimation of the light-induced antimicrobial effect was performed by the incubation of bacteria with AuMs for 1 h in the dark, followed by 1 h illumination. The latter experiments were performed under LED irradiation with 780 nm center wavelength. In all cases, 1 mL of the AuMs solution was inoculated with 1 mL of the bacterial suspension and after 2 h of action aliquots (30 μL) from all samples were subsequently placed on lysogeny broth (LB) agar plates. Bacterial samples incubated in the pristine physiological solutions and without irradiation served as controls. The growth of *E. coli* and *S. epidermidis* was evaluated after 24 h of incubation at 37 °C and the number of colony founded units (CFU) was used as the marker of AuMs antimicrobial activity. All experiments were performed in triplicate.

Acknowledgments

This work was supported by the GACR under the project 15-19485S; Ministry of Health of CR under the projects 15-33459A, 15-33018A, and RFBR 16-33-00351.

Conflict of Interest

The authors declare no conflict of interest.

Keywords: antimicrobial properties · arenediazonium tosylates · light-active nanoparticles · multibranched gold nanoparticles · surface modification

[1] J. M. A. Blair, M. A. Webber, A. J. Baylay, D. O. Ogbolu, L. J. V. Piddock, *Nat. Rev. Microbiol.* **2015**, *13*, 42–51.
[2] F. von Nussbaum, M. Brands, B. Hinzen, S. Weigand, D. Habich, *Angew. Chem. Int. Ed.* **2006**, *45*, 5072–5129; *Angew. Chem.* **2006**, *118*, 5194–5254.
[3] K. M. G. O'Connell, J. T. Hodgkinson, H. F. Sore, M. Welch, G. P. C. Salmond, D. R. Spring, *Angew. Chem. Int. Ed.* **2013**, *52*, 10706–10733; *Angew. Chem.* **2013**, *125*, 10904–10932.
[4] R. Elashnikov, M. Radocha, S. Rimpelova, V. Svorcik, O. Lyutakov, *RSC Adv.* **2015**, *5*, 86825–86831.
[5] N. Cioffi, L. Torsi, N. Ditaranto, G. Tantillo, L. Ghibelli, L. Sabbatini, T. Bleve-Zacheo, M. D'Alessio, P. G. Zambonin, E. Traversa, *Chem. Mater.* **2005**, *17*, 5255–5262.

[6] O. Lyutakov, Y. Kalachyova, A. Solovyev, S. Vytykacova, J. Svanda, J. Siegel, P. Ulbrich, V. Svorcik, *J. Nanopart. Res.* **2015**, *17*, 120.
[7] O. Lyutakov, I. Goncharova, S. Rimpelova, K. Kolarova, J. Svanda, V. Svorcik, *Mater. Sci. Eng. C* **2015**, *49*, 534 – 540.
[8] Y. Suliman, A. Omar, D. Ali, S. Alarifi, A. H. Harrath, L. Mansour, S. H. Alwasel, *Environ. Toxicol.* **2015**, *30*, 149 – 160.
[9] L. Song, M. Connolly, M. L. Fernandez-Cruz, M. G. Vijver, M. Fernandez, E. Conde, G. R. de Snoo, W. J. G. M. Peijnenburg, J. M. Navas, *Nanotoxicology* **2014**, *8*, 383 – 393.
[10] D. Pissuwan, C. H. Cortie, S. M. Valenzuela, M. B. Cortie, *Trends Biotechnol.* **2010**, *28*, 207 – 213.
[11] A. Regiel-Futyra, M. Kus-Liskiewicz, V. Sebastian, S. Irusta, M. Arruebo, G. Stochel, A. Kyziol, *ACS Appl. Mater. Interfaces* **2015**, *7*, 1087 – 1099.
[12] W.-Y. Chen, J.-Y. Lin, W.-J. Chen, L. Luo, E. W.-G. Diau, Y.-C. Chen, *Nanomedicine* **2010**, *5*, 755 – 764.
[13] Y. Zhou, Y. Kong, S. Kundu, J. Cirillo, H. Liang, *J. Nanobiotechnol.* **2012**, *10*, DOI: 10.1186/1477-3155-10-19.
[14] A. Verma, F. Stellacci, *Small* **2010**, *6*, 12 – 21.
[15] L. Vigderman, E. R. Zubarev, *Adv. Drug Delivery Rev.* **2013**, *65*, 663 – 676.
[16] H. Z. Lai, W.-Y. Chen, C.-Y. Wu, Y.-C. Chen, *ACS Appl. Mater. Interfaces* **2015**, *7*, 2046 – 2054.
[17] J. Djafari, C. Marinho, T. Santos, G. Igrejas, C. Torres, J. L. Capelo, P. Poeta, C. Lodeiro, J. Fernandez-Lodeiro, *ChemistryOpen* **2016**, *5*, 206 – 212.
[18] X. Li, S. M. Robinson, A. Gupta, K. Saha, Z. Jiang, D. F. Moyano, A. Sahar, M. A. Riley, V. M. Rotello, *ACS Nano* **2014**, *8*, 10682 – 10686.
[19] Y. Zhao, Z. Chen, Y. Chen, J. Xu, J. Li, X. Jiang, *J. Am. Chem. Soc.* **2013**, *135*, 12940 – 12943.
[20] H. Mu, Q. Liu, H. Niu, Y. Sun, J. Duan, *RSC Adv.* **2016**, *6*, 8714 – 8721.
[21] L. C. Kennedy, L. R. Bickford, N. A. Lewinski, A. J. Coughlin, Y. Hu, E. S. Day, J. L. West, R. A. Drezek, *Small* **2011**, *7*, 169 – 183.
[22] O. Lyutakov, O. Hejna, A. Solovyev, Y. Kalachyova, V. Svorcik, *RSC Adv.* **2014**, *4*, 50624 – 50630.
[23] R. Elashnikov, O. Lyutakov, P. Ulbrich, V. Svorcik, *Mater. Sci. Eng. C* **2016**, *64*, 229 – 235.
[24] C. M. Pitsillides, E. K. Joe, X. Wei, R. R. Anderson, C. P. Lin, *Biophys. J.* **2003**, *84*, 4023 – 4032.
[25] V. P. Zharov, V. Galitovsky, M. Viegas, *Appl. Phys. Lett.* **2003**, *83*, 4897 – 4899.
[26] B. N. Khlebtsov, A. G. Melnikov, V. P. Zharov, N. G. Khlebtsov, *Nanotechnology* **2006**, *17*, 1437 – 1445.
[27] K. C. L. Black, T. S. Sileika, J. Yi, R. Zhang, J. G. Rivera, P. B. Messersmith, *Small* **2014**, *10*, 169 – 178.
[28] M. L. Yin, Z. H. Li, E. G. Ju, Z. Z. Wang, K. Dong, J. S. Ren, X. G. Qu, *Chem. Commun.* **2014**, *50*, 10488 – 10490.
[29] X. Huang, I. H. El-Sayed, W. Qian, M. A. El-Sayed, *J. Am. Chem. Soc.* **2006**, *128*, 2115 – 2120.
[30] T. B. Huff, L. Tong, Y. Zhao, M. N. Hansen, J. X. Cheng, A. Wei, *Nanomedicine* **2007**, *2*, 125 – 132.
[31] C. Loo, A. Lowery, N. J. Halas, J. L. West, R. Drezek, *Nano Lett.* **2005**, *5*, 709 – 711.
[32] E. S. Day, P. A. Thompson, L. Zhang, N. A. Lewinski, N. Ahmed, R. A. Drezek, S. M. Blaney, J. L. West, *J. Neuro-Oncol.* **2011**, *104*, 55 – 63.
[33] J. Chen, C. Claus, R. Laforest, Q. Zhang, M. Yang, M. Gidding, M. Welch, Y. Xia, *Small* **2010**, *6*, 811 – 817.
[34] B. N. Khlebtsov, V. A. Khanadeev, I. L. Maksimova, G. S. Terentyuk, N. G. Khlebtsov, *Nanotechnol. Russia* **2010**, *5*, 454 – 468.
[35] G. S. Terentyuk, G. N. Maslyakova, L. V. Suleymanova, N. G. Khlebtsov, B. N. Khlebtsov, G. G. Akchurin, I. L. Maksimova, V. V. Tuchin, *J. Biomed. Opt.* **2009**, *14*, 021016.
[36] V. P. Zharov, K. E. Mercer, E. N. Galitovskaya, M. S. Smeltzer, *Biophys. J.* **2006**, *90*, 619 – 627.
[37] S. A. Orefuwa, M. Ravanbakhsh, S. N. Neal, J. B. King, A. A. Mohamed, *Organometallics* **2014**, *33*, 439 – 442.
[38] D. M. Shewchuk, M. T. McDermott, *Langmuir* **2009**, *25*, 4556 – 4563.
[39] M. Borzenkov, G. Chirico, L. D'Alfonso, L. Sironi, M. Collini, E. Cabrini, G. Dacarro, C. Milanese, P. Pallavicini, A. Taglietti, C. Bernhard, F. Denat, *Langmuir* **2015**, *31*, 8081 – 8091.
[40] O. A. Guselnikova, M. V. Gromov, A. I. Galanov, *Adv. Mater. Res.* **2014**, *1040*, 309 – 313.
[41] P. S. Postnikov, M. E. Trusova, T. A. Fedushchak, M. A. Uimin, A. E. Ermakov, V. D. Filimonov, *Nanotechnol. Russia* **2010**, *5*, 446 – 449.
[42] A. A. Mohamed, Z. Salmi, S. A. Dahoumane, A. Mekki, B. Carbonnier, M. M. Chehimi, *Adv. Colloid Interface Sci.* **2015**, *225*, 16 – 36.
[43] S. Some, S.-M. Ho, P. Dua, E. Hwang, Y. H. Shin, H. J. Yoo, J.-S. Kang, D.-K. Lee, H. Lee, *ACS Nano* **2012**, *6*, 7151 – 7161.
[44] L. C. Cheng, J. H. Huang, H. M. Chen, T. C. Lai, K. Y. Yang, R. S. Liu, M. Hsiao, C. H. Chen, L. J. He, D. P. Tsai, *J. Mater. Chem.* **2012**, *22*, 2244 – 2253.
[45] K. Kawai, T. Narushima, K. Kaneko, H. Kawakami, M. Matsumoto, A. Hyono, H. Nishihara, T. Yonezawa, *Appl. Surf. Sci.* **2012**, *262*, 76 – 80.
[46] L. Laurentius, S. R. Stoyanov, S. Gusarov, A. Kovalenko, R. Du, G. P. Lopinski, M. T. McDermott, *ACS Nano* **2011**, *5*, 4219 – 4227.
[47] A. Mesnage, X. Lefèvre, P. Jégou, G. Deniau, S. Palacin, *Langmuir* **2012**, *28*, 11767 – 11778.
[48] R. Ahmad, L. Boubekeur-Lecaque, M. Nguyen, S. Lau-Truong, A. Lamouri, P. Decorse, A. Galtayries, J. Pinson, N. Felidj, C. Mangeney, *J. Phys. Chem. C* **2014**, *118*, 19098 – 19105.
[49] F. Hao, C. L. Nehl, J. H. Hafner, P. Nordlander, *Nano Lett.* **2007**, *7*, 729 – 732.
[50] S. Barbosa, A. Agrawal, L. Rodrıguez-Lorenzo, I. Pastoriza-Santos, R. A. Alvarez-Puebla, A. Kornowski, H. Weller, L. M. LizMarzan, *Langmuir* **2010**, *26*, 14943 – 14950.
[51] R. R. Letfullin, C. Joenathan, T. F. George, V. P. Zharov, *Nanomedicine* **2006**, *1*, 473 – 480.
[52] W. C. Huang, P. J. Tsai, Y. C. Chen, *Nanomedicine* **2007**, *2*, 777 – 787.
[53] M. K. Calabretta, A. Kumar, A. M. McDermott, C. Cai, *Biomacromolecules* **2007**, *8*, 1807 – 1811.
[54] R. Benveniste, J. Davies, *Antimicrob. Agents Chemother.* **1973**, *4*, 402 – 409.
[55] D.-J. Guo, F. Mirkhalaf in *Modification of Nano-objects by Aryl Diazonium Salts, in Aryl Diazonium Salts: New Coupling Agents in Polymer and Surface Science* (Ed.: M. M. Chehimi), Wiley-VCH, Weinheim, **2012**, pp. 103 – 124.
[56] V. D. Filimonov, M. E. Trusova, P. S. Postnikov, E. A. Krasnokutskaya, Y. M. Lee, H. Y. Hwang, H. Kim, K.-W. Chi, *Org. Lett.* **2008**, *10*, 3961 – 3964.
[57] O. A. Guselnikova, A. I. Galanov, A. K. Gutakovskii, P. S. Postnikov, *Beilstein J. Nanotechnol.* **2015**, *6*, 1192 – 1198.
[58] A. Adenier, N. Barre, E. Cabet-Deliry, A. Chausse, S. Griveau, F. Mercier, J. Pinson, C. Vautrin, *Surf. Sci.* **2006**, *600*, 4801 – 4812.
[59] J. Pinson, F. Podvorica, *Chem. Soc. Rev.* **2005**, *34*, 429 – 439.
[60] O. Guselnikova, P. Postnikov, R. Elashnikov, M. Trusova, Y. Kalachyova, M. Libansky, J. Barek, Z. Kolska, V. Svorcik, O. Lyutakov, *Colloid Surf. A-Physicochem. Eng.* **2017**, *516*, 274 – 285.
[61] K. Hinrichs, K. Roodenko, J. Rappich, M. M. Chehimi, J. Pinson, in *Aryl Diazonium Salts: New Coupling Agents and Surface Science* (Ed.: M. M. Chehimi), Wiley-VCH, Weinheim, **2012**, p. 83.
[62] J. Lyskawa, D. Belanger, *Chem. Mater.* **2006**, *18*, 4755 – 4763.
[63] H. M. Badawi, W. Förner, S. A. Ali, *Spectrochim. Acta Part A* **2013**, *112*, 388 – 396.
[64] J. Workman, *Handbook of Organic Compounds: IR and Raman Spectra, 1st ed.*, University of Virginia, Academic Press, San Diego, CA, **2000**.

Received: November 28, 2016
Revised: December 28, 2016
Published online on February 7, 2017

